Applied Mathematical Modelling 40 (2016) 10437–10446

Contents lists available at ScienceDirect

Applied Mathematical Modelling

journal homepage: www.elsevier.com/locate/apm

Performance analysis for Feynman's ratchet as a refrigerator with heat leak under different figure of merits

Rui Long*, Baode Li, Wei Liu*

School of Energy and Power Engineering, Huazhong University of Science and Technology, Wuhan 430074, China

ARTICLE INFO

Article history:
Received 9 December 2014
Revised 6 July 2016
Accepted 13 July 2016
Available online 28 July 2016

Keywords:
Feynman's ratchet
refrigerator
heat leak
opitimization

ABSTRACT

The performance of Feynman's ratchet refrigerator with heat leak has been studied under the maximum COP, maximum cooling rate and maximum χ figure of merits. The χ criterion considers both the COP and cooling rate, which can been seen as a trade-off between COP and cooling rate. Therefore the traditional performance region between maximum cooling rate and maximum COP can be divided into two more specific ones (the region between maximum cooling rate and maximum χ, and the region between maximum χ and maximum COP), which represent two different operating demands. The results shows that the operating parameters such as heat leak, external moment, intrinsic energy potential and the Carnot COP have significant impacts on the performance of the Feynman's ratchet refrigerator. If the parameters are properly chosen, the refrigerator can be controlled to operate within the optimal regimes to fulfill the actual specified demands. Furthermore, for given Carnot COP and heat leak, there exist upper bounds for the maximum value of the maximum COP, maximum cooling rate and maximum χ, respectively.

1. Introduction

In classic thermodynamics, the performance of any heat device operating at different heat reservoirs with tempeatures T_h and T_c ($T_h > T_c$) is limited by the Carnot efficiency $\eta_C = 1 - T_c/T_h$ and the Carnot coefficient of performance $\varepsilon_C = T_c/(T_h - T_c)$ for heat engines and refrigerators, respectively. However, to achieve the above two bounds, the thermodynamic cycles should ideally be Carnot ones, where all processes endure with infinite time duration, resulting in no power output for heat engines and no cooling power for refrigerators, and are therefore not able to meet actual demand. Hence cycle duration should be addressed in analyzing the performance of actual heat devices.

By considering the finite time duration of isothermal processes, Curzon-Ahlborn [1] obtained the efficiency of heat engines under the maximum power (MP) condition through the endoreversible Carnot cycle, i.e. the well-known CA efficiency. Based on the CA model, by considering different heat exchanging laws between the working substance, heat reservoirs and the internal dissipations, many revisions have been made to describe the real life heat engines more accurately, and some good results under the maximum power output criterion have been obtained [2–12]. Furthermore, many models have been conceived to investigate the performance of heat engines, such as the low dissipation model [13–15], irreversible heat engines described by the Onsager relations and the extended Onsager relations [16–18], and other thermodynamic models [19–24].

* Corresponding authors. Fax: +86 27 87540724.
E-mail addresses: r_long@hust.edu.cn, 382749412@qq.com (R. Long), w_liu@hust.edu.cn (W. Liu).

http://dx.doi.org/10.1016/j.apm.2016.07.027
0307-904X/

Nomenclature

T	isothermal coefficients
ϕ	intrinsic energy potential
θ	rotation angle per cycle
λ	percentage of the angle for forward jump
ξ	moment
r_0	rate constant
k_B	Boltzmann's constant
R	jump rate, cooling rate
Q	heat
ε	coefficient of performance
σ	heat conductance

Superscripts

+	forward
-	backward
r	reversible

Subscripts

H	hot reservoir
C	cold reservoir
max	maximum

However, minimizing the power consumption could not lead to satisfactory results when attempting to optimize acutal refrigerators [25], and much literature has focused on investigating the performance of refrigerators under different figure of merits [26–29]. Jiménez et al. [30] researched the coefficient of performance of linear irreversible refrigerators under maximum COP figure of merit. Velasco et al. [31] deduced the CA coefficient of performance through endoreversible refrigerators under conditions of maximimum COP per cycle time, that is $\varepsilon_{CA} = \sqrt{\varepsilon_C + 1} - 1$. This is also reported in a later model with non-isothermal processes [26]. To include the energy benefits and losses, Hernandez et al. [32] brought forward the Ω criterion, and attention have been focused on optimizing different refrigerators based on the Ω figure of merit. Under this criterion, De Tomas et al. [33] and Hu et al. [34] deduced the upper and lower COP bounds through the low dissipation models. These are also obtained through the minimally nonlinear irreversible refrigerator model [35]. Later, the χ figure of merit, which considers both the COP and the cooling rate, was conceived to optimize actual refrigerators [36,37]. Wang et al. [25] deduced the COP bounds for low dissipation refrigerators at maximum χ figure of merit. These are in close agreement with experimental data for actual refrigerators.

Feynman, in his celebrated lectures, introduced an imaginary ratchet device that can work as a heat engine as well as a refrigerator [38]. Many discussions have taken place around this device [22,39–44], and the performance for Feynman's ratchet as a heat engine has been studied [40,45,46]. As a counterpart, in this paper, we systematically investigate the performance of Feynman's ratchet as a refrigerator under different criteria (maximum COP, maximum cooling rate and maximum χ figure of merits), and heat leak between the heat reservoirs has been considered. The general expressions of several important parameters of the refrigerator - COP, cooling load rate, and the χ objective function - have been derived. The impacts of some of these main parameters on the performance of the refrigerator have been analyzed in detail. Some results, which reveal the general performance characteristics, are obtained. These results may prove helpful in understanding the performance characteristics of Feynman's ratchet as a refrigerator.

2. Mathematical model

The traditional model of Feynman's ratchet consists of a ratchet, a pawl and spring, vanes, two heat reservoirs at temperatures $T_C < T_H$, an axle and wheel, and the load. The vane is immersed in the hot reservoir and the ratchet in the cold reservoir. The Feynman's ratchet refrigerator cycle can be treated as an inversed cycle of the Feynman's ratchet heat engine. The ratchet potential is schematically depicted in Fig. 1.

The intrinsic energy potential is denoted as ϕ. θ is the rotation angle per cycle and λ represents the percentage of the angle for forward jump ($0 < \lambda < 1$). The heat is pulled from the cold reservoir (left) to the hot reservoir (right) by a moment, ξ, due to the external moment. The energy needed for a forward jump is $\phi - \xi\lambda\theta$ and for a backward jump is $\phi + \xi(1-\lambda)\theta$. We assume the rates of both forward and backward jumps are proportional to the corresponding Arrhenius factor [38], and can be expressed respectively as

$$R^+ = r_o e^{-(\phi - \xi\lambda\theta)/T_C k_B} \tag{1}$$

$$R^- = r_o e^{-(\phi + \xi(1-\lambda)\theta)/T_H k_B}, \tag{2}$$

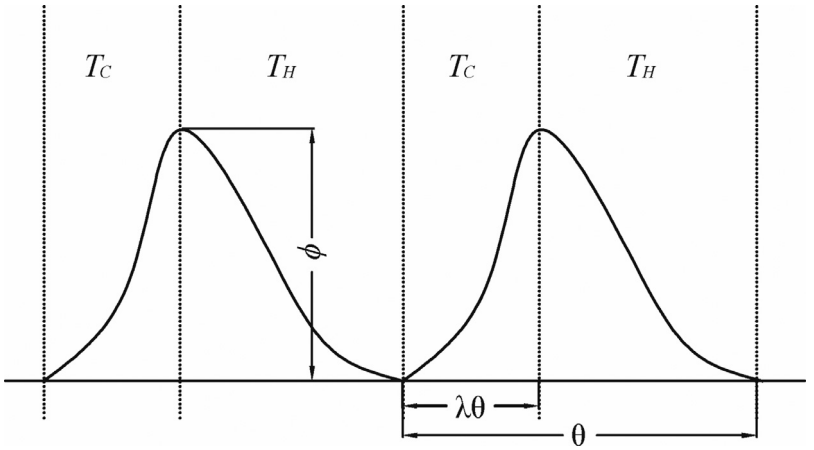

Fig. 1. Potential energy as a function of the rotation angle of the ratchet.

where r_0 is a rate constant with the dimension $1/s$, and k_B is Boltzmann's constant. In forward and back steps, the heat absorbed and released from the heat reservoirs per unit time are given by

$$\dot{Q}_C^r = r_o(\phi - \xi\lambda\theta)\left[e^{-(\phi-\xi\lambda\theta)/T_C k_B} - e^{-(\phi\varepsilon+\xi(1-\lambda)\theta)/T_H k_B}\right] \tag{3}$$

$$\dot{Q}_H^r = r_o[\phi + \xi(1-\lambda)\theta]\left[e^{-(\phi-\xi\lambda\theta)/T_C k_B} - e^{-(\phi+\xi(1-\lambda)\theta)/T_H k_B}\right]. \tag{4}$$

In this paper, the heat flow from the hot reservoir to the cold reservoir through the axle is considered, and obeys the Fourier law with heat conductance σ. Then, heat leak from the hot reservoir to the cold reservoir can be written as

$$\dot{Q}_{leak} = \sigma(T_H - T_C). \tag{5}$$

Therefore, the rate of total heat transferred from the cold reservoir is

$$\dot{Q}_C = \dot{Q}_C^r - \dot{Q}_{leak}, \tag{6}$$

and the rate of total heat transferred to the hot reservoir is

$$\dot{Q}_H = \dot{Q}_H^r - \dot{Q}_{leak}. \tag{7}$$

It is clear that heat leak does not affect the power input. The COP and the cooling load rate (R) are

$$\varepsilon = \frac{\dot{Q}_C}{\dot{Q}_H - \dot{Q}_C} = \frac{r_o(\phi - \xi\lambda\theta)\left[e^{-(\varepsilon\phi-\xi\lambda\theta)/T_C k_B} - e^{-(\phi+\xi(1-\lambda)\theta)/T_H k_B}\right] - \sigma(T_H - T_C)}{r_o\xi\theta\left[e^{-(\phi-\xi\lambda\theta)/T_C k_B} - e^{-(\phi+\xi(1-\lambda)\theta)/T_H k_B}\right]} \tag{8}$$

$$R = r_o(\phi - \xi\lambda\theta)\left[e^{-(\phi-\xi\lambda\theta)/T_C k_B} - e^{-(\phi+\xi(1-\lambda)\theta)/T_H k_B}\right] - \sigma(T_H - T_C). \tag{9}$$

In order to discuss simply, we can rewrite Eqs. (8) and (9) in a dimensionless form, thus

$$\varepsilon = \frac{\phi*}{x} - \lambda - \frac{\sigma*}{x}\frac{1}{\varepsilon_C + 1}\left[e^{-\frac{\varepsilon_C+1}{\varepsilon_C}(\phi^* - \lambda x)} - e^{-(\phi^* + (1-\lambda)x)}\right]^{-1} \tag{10}$$

$$R^* = \frac{R}{r_O K_B T_H} = (\phi^* - \lambda x)\left[e^{-\frac{\varepsilon_C+1}{\varepsilon_C}(\phi^* - \lambda x)} - e^{-(\phi^* + (1-\lambda)x)}\right] - \sigma^*\frac{1}{\varepsilon_C + 1}, \tag{11}$$

where

$$\phi^* = \frac{\phi}{k_B T_H}, \quad x = \frac{\xi\theta}{k_B T_H}, \quad \sigma^* = \frac{\sigma}{r_O k_B}. \tag{12}$$

Furthermore, the dimensionless χ function can be rewritten as $\chi^* = \varepsilon R^*$. To drive the refrigerator, $R^+ > R^-$, so then $x > \phi^*/(\varepsilon_C + \lambda)$. Based on the above equations, we will systematically investigate the performance of Feynman's ratchet as a refrigerator under different criteria (maximum COP, maxmium cooling rate and maximum χ figure of merits) in the following discussion.

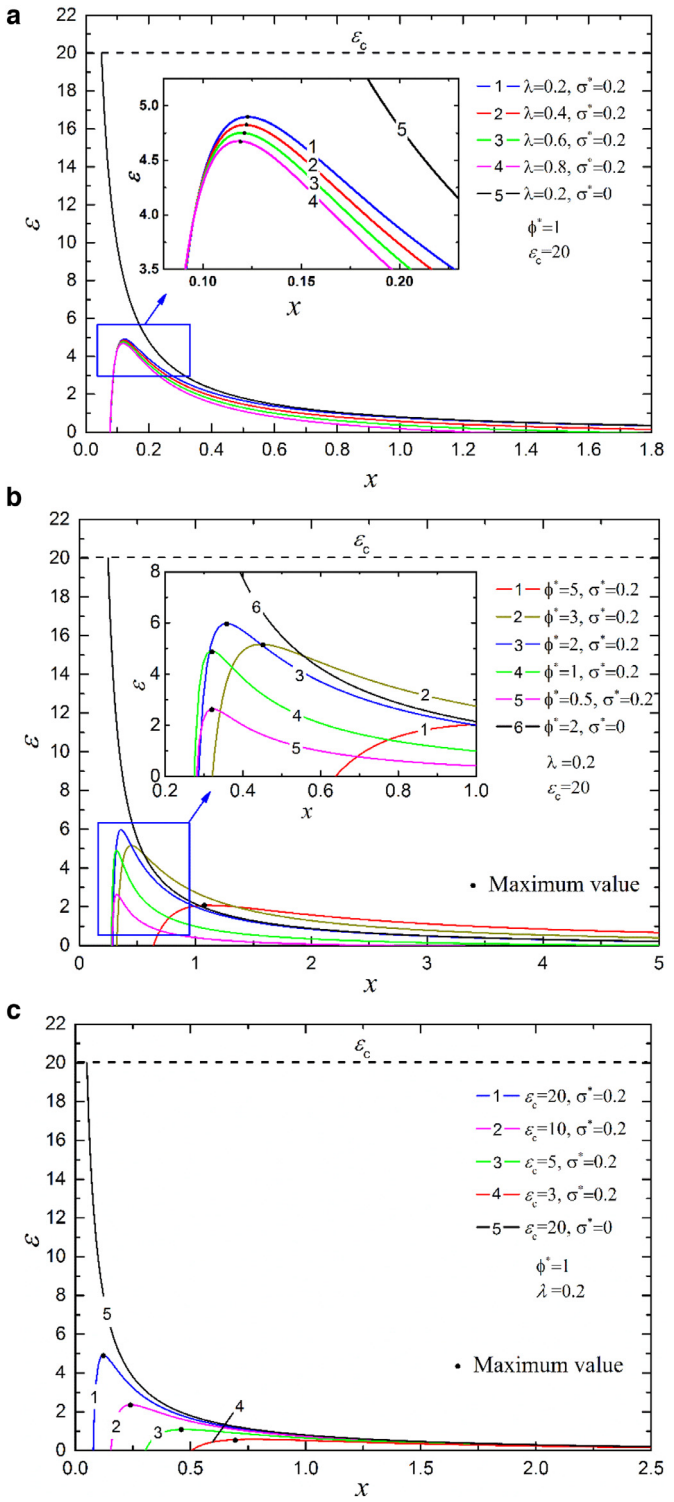

Fig. 2. The curves of the COP varying with the dimensionless external moment x for a set of given parameters.

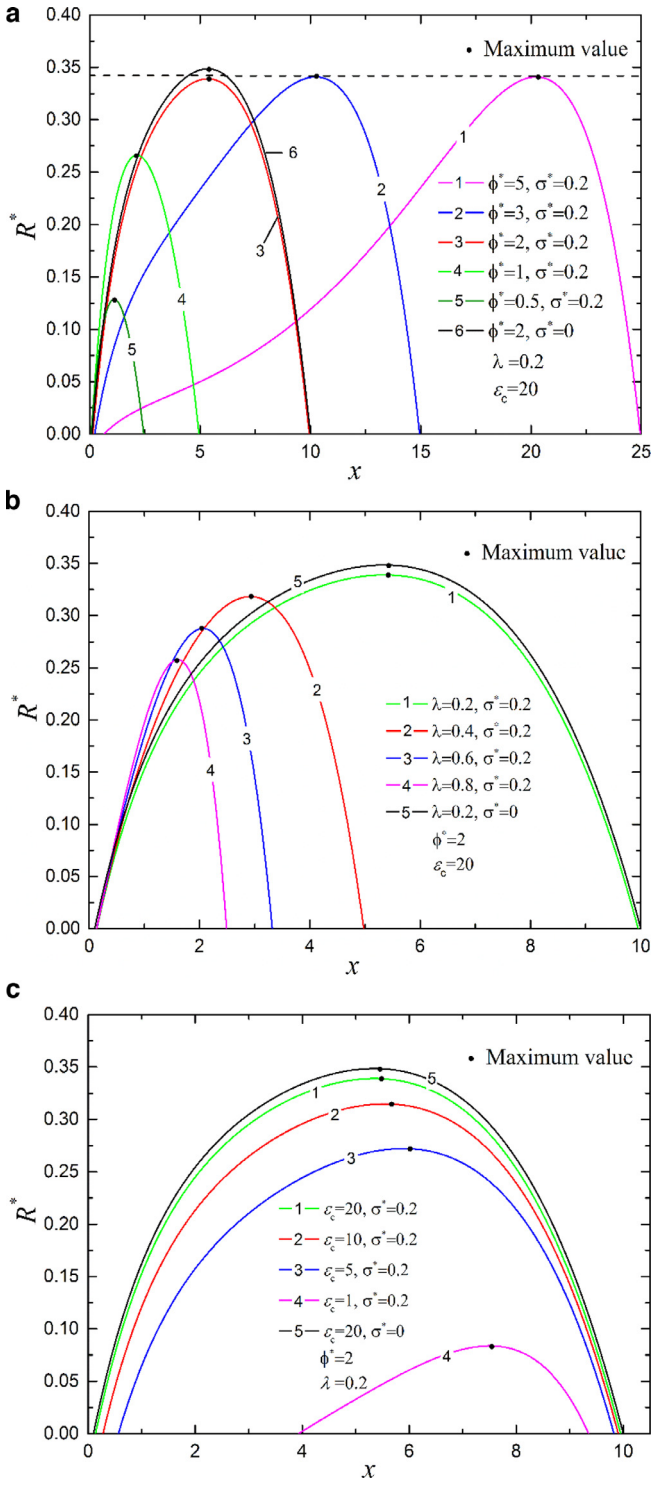

Fig. 3. The curves of the cooling rate varying with the dimensionless external moment x for a set of given parameters.

3. The impact of parameters on performance

Using Eq. (10), we can generate the curves of COP versus x with given parameters $\sigma*$, $\phi*$ and λ. As shown in Fig. 2, when the dimensionless heat conductance is absent, the curves of COP versus x are hyperbolic ones. COP decreases with increasing x monotonously. With the presence of heat leak, the curves become parabolic, and there exists an optimal external moment

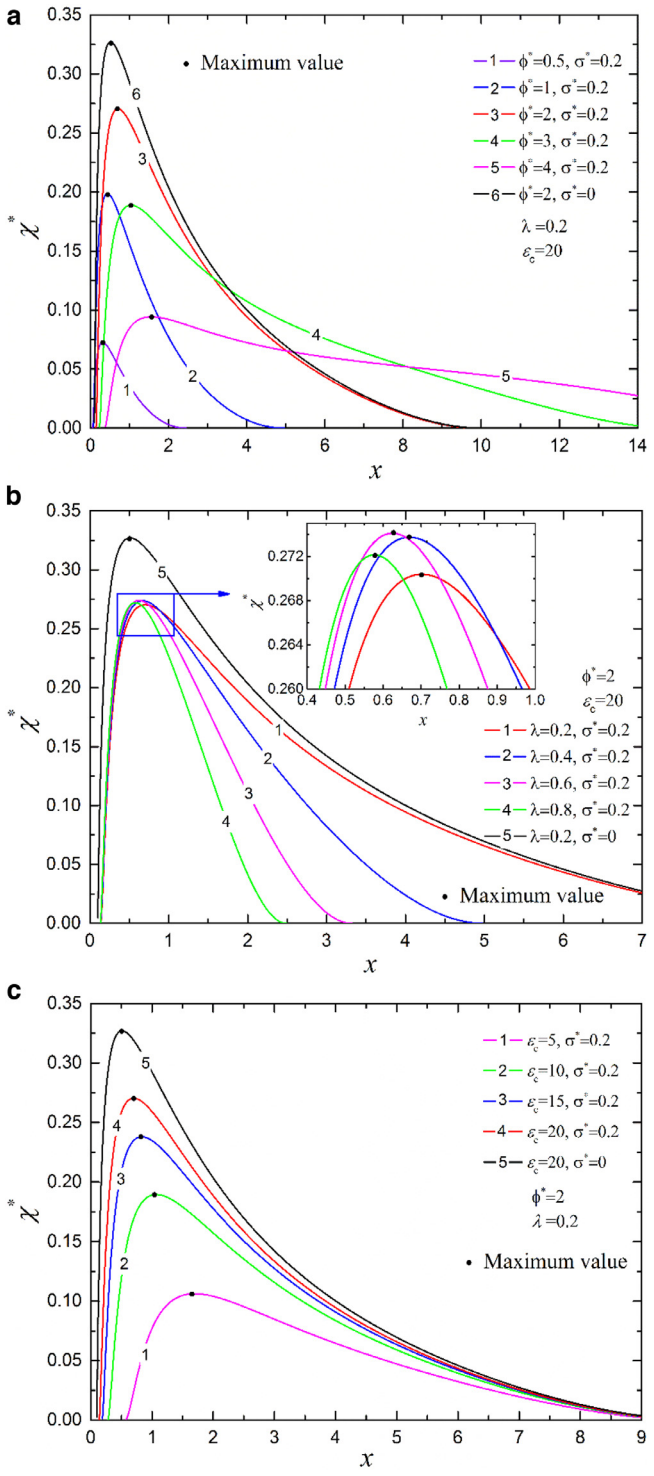

Fig. 4. The curves of the value of $\chi*$ varying with the dimensionless external moment x.

($x_{max,\varepsilon}$) corresponding to the maximum COP (ε_{max}). The COP vanishes at certain low and high values of x, respectively. The values of $x_{max,\varepsilon}$ and ε_{max} depend on the parameters $\sigma*$, $\phi*$, λ and ε_C. In addition, the maximum COP (ε_{max}) increases with decreasing λ and increasing ε_C. However, ε_{max} first increases with increasing $\phi*$, then decreases, as depicted in Fig. 2(b). Furthermore, $x_{max,\varepsilon}$ decreases with increasing ε_C and $\phi*$. However, it increases with increasing λ.

In Fig. 3, we can see that regardless of whether heat leak is considered or not, the curves are parabolic. The existence of heat leak will reduce the cooling rate. There exists an optimal external moment ($x_{max,R*}$) corresponding to the maximum

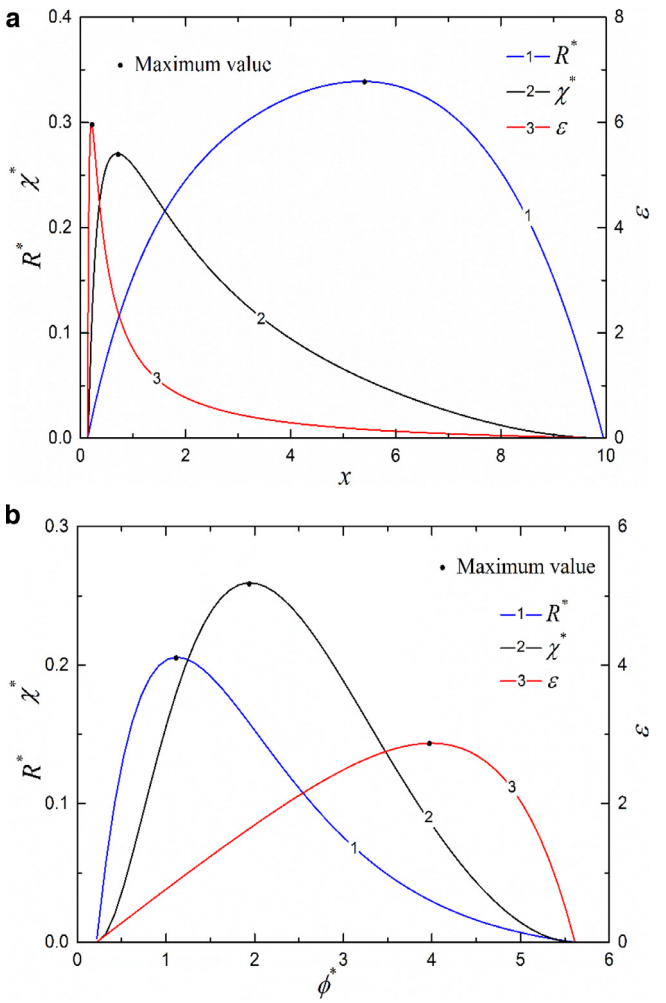

Fig. 5. The influences of x and on the cooling rate, the values of and COP with prescribed parameters: (a), and (b).

cooling rate ($R*_{max}$). In Fig. 3(b) and (c), the maximum cooling rate ($R*_{max}$) increases with decreasing λ and increasing ε_C. However, when $\phi*$ is larger than a certain value, $R*_{max}$ will achieve its maximum value and stay constant, and will be independent of $\phi*$, as depicted in Fig. 3(a). It is also clear that x_{max,R^*} increases with decreasing λ and ε_C; however it increases with increasing $\phi*$. When $\phi*$ is larger than a certain value, $R*_{max}$ stays constant, but x_{max,R^*} still increases with $\phi*$. Their physical meanings are very clear. The energy needed for a forward jump is $\phi - \xi\lambda\theta$ and for a backward jump is $\phi + \xi(1-\lambda)\theta$. A larger value of λ results in a smaller value of $\dot{Q}_C$. Thus when λ is increased, both the cooling rate and COP will decrease. Furthermore, when $\phi*$ increases, the energy absorbed per jump will increase and $R^+ - R^-$ will decrease. At higher $\phi*$, the increase impact on $R^+ - R^-$ will compensate for the increase impact on $\phi - \xi\lambda\theta$; therefore $R*_{max}$ stays constant.

The χ criterion is the product of the COP and the cooling rate, so both the two important performance parameters (COP and the cooling rate) are considered. In Fig. 4, we can see that regardless of whether heat leak is considered or not, the curves are parabolic and the existence of heat leak will reduce the values of $\chi*$. There exists an optimal external moment (x_{max,χ^*}) corresponding to the maximum value (χ^*_{max}) of $\chi*$. As shown in Fig. 4(a) and 4(b), χ^*_{max} first increases with $\phi*$ and λ, then decreases. But it monotonously increases with increasing ε_C, as depicted in Fig. 4(c). The optimal external moment (x_{max,χ^*}) increases with increasing $\phi*$, while it decreases with increasing λ and ε_C.

The impacts of x and $\phi*$ on the cooling rate, the values of $\chi*$ and COP are also presented in Fig. 5. The cooling rate, the values of $\chi*$ and COP all first increase with x and $\phi*$, then decrease, as shown in Fig. 5(a) and (b). There also exist optimal intrinsic energy potentials ($\phi^*_{max,\varepsilon}$, ϕ^*_{max,R^*} and ϕ^*_{max,χ^*}, respectively) that correspond to the maximum COP, maximum cooling rate and the maximum value of $\chi*$. In Fig. 5 (a), for given parameters $\sigma*$, λ, $\phi*$ and ε_C, we have $x_{max,\varepsilon} < x_{max,\chi^*} < x_{max,R^*}$. And for given parameters $\sigma*$, λ, x and ε_C, we have $\phi^*_{max,R^*} < \phi^*_{max,\chi^*} < \phi^*_{max,\varepsilon}$, as shown in Fig. 5(b).

Based on Eqs. (10)–(11) and the definition of χ, we can obtain the cooling rate and the value of χ versus COP characteristics, as shown in Fig. 6. We can see that, when heat leak is present, the curves of $R*$ versus ε and $\chi*$ versus ε are

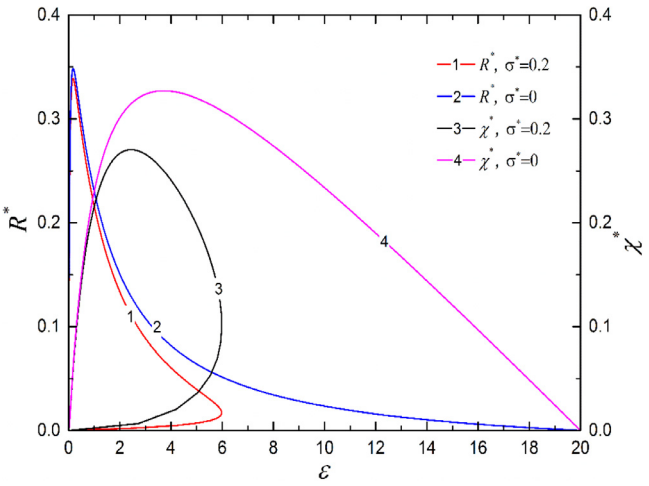

Fig. 6. The curves of the cooling rate and the χ objective function varying with COP (and).

prarabolic. The curves become loop-shaped when heat leak is considered. Furthermore, heat leak will reduce the COPs corresponding to the maximum cooling rate and $\chi*$, respectively. In addition, as depicted in Fig. 6, for given parameters, we have $\varepsilon_{\max,R^*} < \varepsilon_{\max,\chi} < \varepsilon_{\max}$ and $R^*_{\max,\varepsilon} < R^*_{\max,\chi} < R^*_{\max}$, where $R^*_{\max,\varepsilon}$ and $R^*_{\max,\chi}$ are the cooling rates corresponding to the maximum COP and χ figure of merits, respectively.

4. Optimal operating regions

Usually for a refrigerator, the aim is to obtain the cooling load and COP as large as possible for a given set of other parameters. However, a larger cooling load will lead to a lower COP. The χ criterion considers both the COP and cooling rate. We can treat it as a trade-off figure of merit between the COP and cooling rate criteria. Therefore the traditional performance region between maximum cooling rate and maximum COP can be divided into two more specific performance regions (the region between maximum cooling rate and maximum χ, and the region between maximum χ and maximum COP). These two performance regions represent two different operating demands. If the main demand is cooling rate and energy saving is not so important, it is therefore more reasonable for the Feynman's ratchet refrigerator to operate under the performance of maximum cooling rate and maximum χ figure of merit. That is to say, the dimensionless external moment, intrinsic energy potential and the COP should be, respectively, located in

$$x_{max,\chi^*} < x < x_{max,R^*}, \quad \phi^*_{max,R^*} < \phi^* < \phi^*_{max,\chi^*}, \quad \varepsilon_{\max,R^*} < \varepsilon < \varepsilon_{\max,\chi}. \tag{13}$$

In this region, the cooling rate will decrease with increasing COP, while the χ figure of merit will increase with COP. The optimal external moment and the intrinsic energy potential should be located in the regions

$$k_B T_H x_{\max,\chi^*}/\theta < \xi < k_B T_H x_{\max,R^*}/\theta, k_B T_H \phi^*_{\max,R^*} < \phi < k_B T_H \phi^*_{\max,\chi^*}. \tag{14}$$

If the main demand is energy saving, but the cooling rate should also be considered, it is more reasonable for the Feynman's ratchet refrigerator to operate under the conditions of maximum χ figure of merit and maximum COP. That is to say, the dimensionless external moment and intrinsic energy potential should be, respectively, located in

$$x_{max,\varepsilon} < x < x_{max,\chi^*}, \phi^*_{max,\chi^*} < \phi^* < \phi^*_{max,\varepsilon}, \varepsilon_{\max,\chi} < \varepsilon < \varepsilon_{\max}. \tag{15}$$

In this region, both the cooling rate and the χ figure of merit will decrease with increasing COP. The optimal external moment and the intrinsic energy potential should be located in the regions

$$k_B T_H x_{max,\varepsilon}/\theta < \xi < k_B T_H x_{max,\chi^*}/\theta, k_B T_H \phi^*_{max,\chi^*} < \phi < k_B T_H \phi^*_{max,\varepsilon}. \tag{16}$$

5. Maximum cooling rate, maximum COP and maximum χ

The maximum cooling rate, maximum COP and maximum χ versus the external moment and the intrinsic energy potential are illustrated, respectively, in Fig. 7. It can be seen that the maximum cooling load is a monotonic increasing function of the external moment and the intrinsic energy potential, which then tends to stay at a fixed value as the external moment and the the intrinsic energy potential increase. The maximum COP and maximum χ both first increase with increasing external moment and intrinsic energy potential, then decrease. There exist optimum external moments and intrinsic energy potentials corresponding to the maximum values of ε_{max} and χ^*_{max}, respectively. Furthermore,

$$x_{\max,\varepsilon_{max}} < x_{\max,\chi^*_{max}} < x_{\max,R^*_{max}}, \quad \phi^*_{\max,\chi^*_{max}} < \phi^*_{\max,\varepsilon_{max}} < \phi^*_{\max,R^*_{max}}, \tag{17}$$

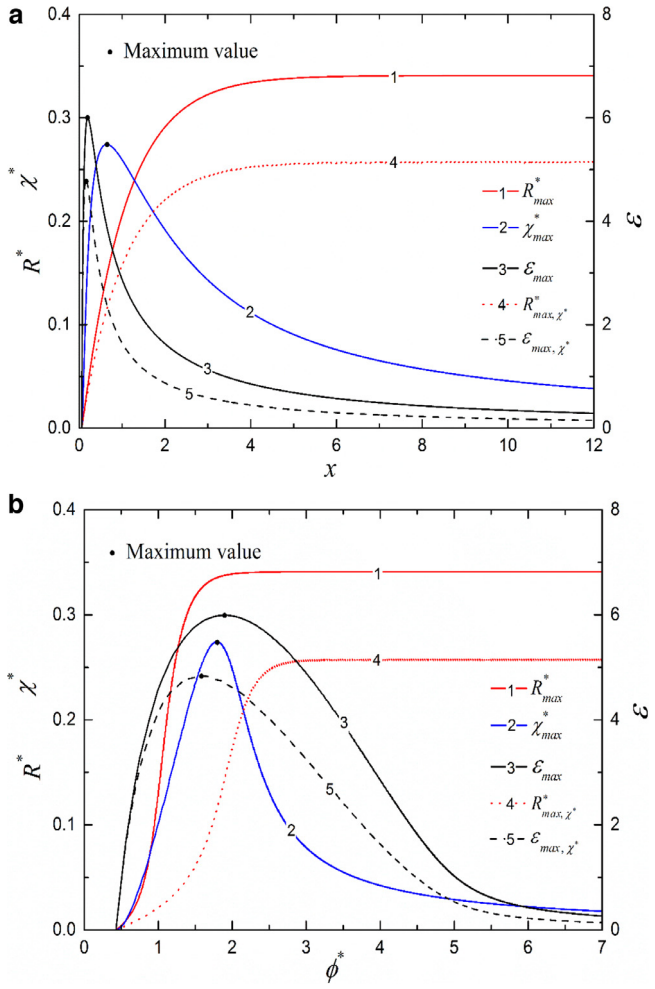

Fig. 7. The influences of x (a) and $\phi*$ (b) on the maximum cooling rate and maximum (and).

where $x_{\max,\varepsilon_{max}}$, $x_{\max,\chi^*_{max}}$, $\phi^*_{\max,\varepsilon_{max}}$ and $\phi^*_{\max,\chi^*_{max}}$ are the external moment and intrinsic energy potential corresponding to the upper bounds of the maximum COP and χ, respectively. $x_{\max,R^*_{max}}$ and $\phi^*_{\max,R^*_{max}}$ are the minimum external moment and intrinsic energy potential corresponding to the upper bound of the maximum cooling rate.

6. Conclusions

The performance of Feynman's ratchet as a refrigerator with heat leak has been studied, based on the maximum COP, maximum cooling rate and maximum χ figure of merits. The χ figure of merit considers both the COP and cooling rate. It can been seen as a trade-off between COP and cooling rate. The results show that with the existance of heat leak, the COP can never achieve the Carnot COP. Similar to the charateristics of real conventional refrigerators and the thermal Brownian refrigerator [47], the cooling load versus COP charateristics are closed loop-shaped curves, as too are the characteristics of χ versus COP. The operating parameters such as heat leak, external moment, intrinsic energy potential and the Carnot COP have significant impacts on the performance of the Feynman's ratchet refrigerator. Furthermore, we divide the traditional performance region between maximum cooling rate and maximum COP into two more specific performance regions (the region between maximum cooling rate and maximum χ, and the region between maximum χ and maximum COP). These two performance regions represent two different operating demands. If parameters are properly chosen, the refrigerator can be controlled to operate in different optimal regimes to fulfill the specified demands. Furthermore, there exists an upper bound for maximum value of ε_{max} R^*_{max} and χ^*_{max}. So for the prescribed heat leak and Carnot COP, we can choose the appropriate external momentum and intrinsic energy potential to make the refrigerator operate under the maximum different demands.

Acknowledgments

The work was supported by the National Key Basic Research Program of China (973 Program) (2013CB228302).

References

[1] F.L. Curzon, B. Ahlborn, Efficiency of a Carnot engine at maximum power output, Am. J. Phys. 43 (1) (1975) 22.
[2] L. Chen, F. Sun, C. Wu, Effect of heat transfer law on the performance of a generalized irreversible Carnot engine, J. Phys. D: Appl. Phys. 32 (2) (1999) 99.
[3] L. Chen, Z. Yan, The effect of heat-transfer law on performance of a two-heat-source endoreversible cycle, J. Chem. Phys. 90 (7) (1989) 3740.
[4] Z. Yan, J. Chen, Optimal performance of a generalized Carnot cycle for another linear heat transfer law, J. Chem. Phys. 92 (3) (1990) 1994.
[5] C. Wu, R.L. Kiang, Finite-time thermodynamic analysis of a Carnot engine with internal irreversibility, Energy 17 (12) (1992) 1173–1178.
[6] J. Chen, The maximum power output and maximum efficiency of an irreversible Carnot heat engine, J. Phys. D: Appl. Phys. 27 (6) (1994) 1144.
[7] P. Salamon, Finite time optimizations of a Newton's law Carnot cycle, J. Chem. Phys. 74 (6) (1981) 3546.
[8] J. Gonzalez-Ayala, L.A. Arias-Hernandez, F. Angulo-Brown, Connection between maximum-work and maximum-power thermal cycles, Phys. Rev. E 88 (5) (2013) 052142.
[9] F. Angulo-Brown, R. Paéz-Hernańdez, Endoreversible thermal cycle with a nonlinear heat transfer law, J. Appl. Phys. 74 (4) (1993) 2216.
[10] J. Gordon, M. Huleihil, General performance characteristics of real heat engines, J. Appl. Phys. 72 (3) (1992) 829–837.
[11] H. Song, L. Chen, J. Li, F. Sun, C. Wu, Optimal configuration of a class of endoreversible heat engines with linear phenomenological heat transfer law [q∝Δ(T[sup −1])], J. Appl. Phys. 100 (12) (2006) 124907.
[12] A. Bejan, Entropy generation minimization: the new thermodynamics of finite-size devices and finite-time processes, J. Appl. Phys. 79 (3) (1996) 1191.
[13] J. Wang, J. He, Efficiency at maximum power output of an irreversible Carnot-like cycle with internally dissipative friction, Phys. Rev. E 86 (5) (2012) 051112.
[14] Y. Wang, Z.C. Tu, Efficiency at maximum power output of linear irreversible Carnot-like heat engines, Phys. Rev. E 85 (1) (2012) 011127.
[15] J. Guo, J. Wang, Y. Wang, J. Chen, Universal efficiency bounds of weak-dissipative thermodynamic cycles at the maximum power output, Phys. Rev. E 87 (1) (2013) 012133.
[16] C. Van den Broeck, Thermodynamic efficiency at maximum power, Phys. Rev. Lett. 95 (19) (2005) 190602.
[17] L. Onsager, Reciprocal relations in irreversible processes. I, Phys. Rev. 37 (4) (1931) 405–426.
[18] Y. Izumida, K. Okuda, Efficiency at maximum power of minimally nonlinear irreversible heat engines, EPL (Europhys. Lett.) 97 (1) (2012) 10004.
[19] R. Long, W. Liu, Unified trade-off optimization for general heat devices with nonisothermal processes, Phys. Rev. E 91 (4) (2015) 042127.
[20] L. Chen, C. Wu, F. Sun, Finite time thermodynamic optimization or entropy generation minimization of energy systems, J. Non-Equilib. Thermodyn. 24 (4) (1999) 327–359.
[21] R. Long, W. Liu, Performance of micro two-level heat devices with prior information, Phys. Lett. A 379 (36) (2015) 1979–1982.
[22] Z.-M. Ding, L.-G. Chen, W.-H. Wang, Y.-L. Ge, F.-R. Sun, Exploring the operation of a microscopic energy selective electron engine, Physica A 431 (2015) 94–108.
[23] R. Long, W. Liu, Ecological optimization for general heat engines, Phys. Stat. Mech. Appl. (2015) 232–239.
[24] Z.M. Ding, L.G. Chen, W.H. Wang, F.R. Sun, Progress in study on finite time thermodynamic performance optimization for three kinds of microscopic energy conversion systems, Sci. Sin. 45 (9) (2015) 889–918.
[25] Y. Wang, M. Li, Z.C. Tu, A.C. Hernández, J.M.M. Roco, Coefficient of performance at maximum figure of merit and its bounds for low-dissipation Carnot-like refrigerators, Phys. Rev. E 86 (1) (2012) 011127.
[26] R. Long, W. Liu, Coefficient of performance and its bounds for general refrigerators with nonisothermal processes, J. Phys. A: Math. Theor. 47 (32) (2014) 325002.
[27] R. Long, W. Liu, Ecological optimization and coefficient of performance bounds of general refrigerators, Physica A 443 (2016) 14–21.
[28] R. Long, W. Liu, Coefficient of performance and its bounds with the figure of merit for a general refrigerator, Phys. Scr. 90 (2) (2015) 025207.
[29] R. Long, W. Liu, Performance of quantum Otto refrigerators with squeezing, Phys. Rev. E 91 (6) (2015) 062137.
[30] B. Jiménez de Cisneros, L. Arias-Hernández, A. Hernández, Linear irreversible thermodynamics and coefficient of performance, Phys. Rev. E 73 (5) (2006) 057103.
[31] S. Velasco, J.M.M. Roco, A. Medina, A.C. Hernández, New performance bounds for a finite-time carnot refrigerator, Phys. Rev. Lett. 78 (17) (1997) 3241–3244.
[32] A.C. Hernández, A. Medina, J. Roco, J. White, S. Velasco, Unified optimization criterion for energy converters, Phys. Rev. E 63 (3) (2001) 037102.
[33] C. de Tomas, J.M.M. Roco, A.C. Hernández, Y. Wang, Z.C. Tu, Low-dissipation heat devices: unified trade-off optimization and bounds, Phys. Rev. E 87 (1) (2013) 012105.
[34] Y. Hu, F. Wu, Y. Ma, J. He, J. Wang, A. Hernández, et al., Coefficient of performance for a low-dissipation Carnot-like refrigerator with nonadiabatic dissipation, Phys. Rev. E 88 (6) (2013) 062115.
[35] R. Long, Z. Liu, W. Liu, Performance optimization of minimally nonlinear irreversible heat engines and refrigerators under a trade-off figure of merit, Phys. Rev. E 89 (6) (2014) 062119.
[36] Z. Yan, J. Chen, A class of irreversible Carnot refrigeration cycles with a general heat transfer law, J. Phys. D: Appl. Phys 23 (2) (1990) 136.
[37] C. de Tomás, A.C. Hernández, J.M.M. Roco, Optimal low symmetric dissipation Carnot engines and refrigerators, Phys. Rev. E 85 (1) (2012) 010104.
[38] R. Feynman, R. Leighton, M. Sands, The Feynman Lectures on Physics, 1, Addison-Wesley, Reading, MA, 1963.
[39] Z.C. Tu, Efficiency at maximum power of Feynman's ratchet as a heat engine, J. Phys. A: Math. Theor 41 (31) (2008) 312003.
[40] S. Velasco, J. Roco, A. Medina, A.C. Hernández, Feynman's ratchet optimization: maximum power and maximum efficiency regimes, J. Phys. D: Appl. Phys. 34 (6) (2001) 1000.
[41] C. Jarzynski, O. Mazonka, Feynman's ratchet and pawl: an exactly solvable model, Phys. Rev. E 59 (6) (1999) 6448.
[42] K. Sekimoto, Kinetic characterization of heat bath and the energetics of thermal ratchet models, J. Phys. Soc. Jpn 66 (66) (1997) 1234–1237.
[43] H. Sakaguchi, Fluctuation theorem for a langevin model of the feynman ratchet, J. Phys. Soc. Jpn 69 (1) (2000) 104–108.
[44] L. Chen, Z. Ding, F. Sun, Optimum performance analysis of Feynman's engine as cold and hot ratchets, J. Non-Equilib. Thermodyn. 36 (2) (2011) 155–177.
[45] T. Hondou, F. Takagi, Irreversible Operation in a Stalled State of Feynman's Ratchet, J. Phys. Soc. Jpn 67 (9) (1998) 2974–2976.
[46] M.O. Magnasco, G. Stolovitzky, Feynman's Ratchet and Pawl, J. Stat. Phys. 93 (3-4) (1998) 615–632.
[47] L. Chen, Z. Ding, F. Sun, A generalized model of an irreversible thermal Brownian refrigerator and its performance, Appl. Math. Modell. 35 (6) (2011) 2945–2958.